

## Durham Research Online

---

### Deposited in DRO:

23 May 2017

### Version of attached file:

Accepted Version

### Peer-review status of attached file:

Peer-reviewed

### Citation for published item:

Rogerson, M. and Mercedes-Martin, R. and Brasier, A.T. and McGill, R.A.R. and Prior, T.J. and Vonhof, H. and Fellows, S.M. and Reijmer, J.J.G. and McClymont, E.L. and Billing, I. and Matthews, A. and Pedley, M. (2017) 'Are spherulitic lacustrine carbonates an expression of large-scale mineral carbonation? A case study from the East Kirkton Limestone, Scotland.', *Gondwana research.*, 48 . pp. 101-109.

### Further information on publisher's website:

<https://doi.org/10.1016/j.jgr.2017.04.007>

### Publisher's copyright statement:

© 2017 This manuscript version is made available under the CC-BY-NC-ND 4.0 license  
<http://creativecommons.org/licenses/by-nc-nd/4.0/>

### Additional information:

## Use policy

---

The full-text may be used and/or reproduced, and given to third parties in any format or medium, without prior permission or charge, for personal research or study, educational, or not-for-profit purposes provided that:

- a full bibliographic reference is made to the original source
- a [link](#) is made to the metadata record in DRO
- the full-text is not changed in any way

The full-text must not be sold in any format or medium without the formal permission of the copyright holders.

Please consult the [full DRO policy](#) for further details.

Are Spherulitic Lacustrine Carbonates an Expression of Large-Scale Mineral Carbonation? A case study from the East Kirkton Limestone, Scotland.

Mike Rogerson<sup>1</sup>, Ramon Mercedes-Martín<sup>1</sup>, Alexander T. Brasier<sup>2</sup>, Rona A.R. McGill<sup>3</sup>, Tim J. Prior<sup>4</sup>, Hubert Vonhof<sup>5</sup>, Simon M. Fellows<sup>4</sup>, John J. G. Reijmer<sup>6</sup>, Erin McClymont<sup>7</sup>, Ian Billing<sup>8,9</sup>, Anna, Matthews<sup>8</sup> and Martyn Pedley<sup>1</sup>

1. Department of Geography, Environment and Earth Sciences, University of Hull, Cottingham Road, Hull, UK. HU6 7RX. Tel. +44 (0)1482466051. [m.rogerson@hull.ac.uk](mailto:m.rogerson@hull.ac.uk); [r.mercedes@hull.ac.uk](mailto:r.mercedes@hull.ac.uk); [h.m.Pedley@hull.ac.uk](mailto:h.m.Pedley@hull.ac.uk)

2. School of Geosciences, Meston Building, University of Aberdeen, Old Aberdeen, Scotland, UK. AB24 3UE. Tel. +44(0)1224273449. [a.brasier@abdn.ac.uk](mailto:a.brasier@abdn.ac.uk)

3. Scottish Universities Environmental Research Centre (SUERC), Rankine Avenue, East Kilbride G75 0QF. Tel. +44(0) 01355270158. [Rona.McGill@glasgow.ac.uk](mailto:Rona.McGill@glasgow.ac.uk)

4. Department of Chemistry, University of Hull, Cottingham Road, Hull, UK. HU6 7RX. Tel. +44(0)1482466389. [t.prior@hull.ac.uk](mailto:t.prior@hull.ac.uk); [s.m.fellows@hull.ac.uk](mailto:s.m.fellows@hull.ac.uk)

5. Max Planck Institute of Chemistry, Hahn-Meitnerweg 1, 55128, Mainz Germany. Tel +4961313056605. [hubert.vonhof@mpic.de](mailto:hubert.vonhof@mpic.de)

20 6. Faculty of Earth and Life Sciences, Vrije Universiteit Amsterdam, De Boelelaan 1085,  
21 1081HV, Amsterdam, The Netherlands. 1081HV. Tel. +31 20 59 87360. h.b.vonhof@vu.nl;  
22 j.j.g.reijmer@vu.nl

23 7 Department of Geography , Durham University , Lower Mountjoy , South Road, Durham ,  
24 DH1 3LE, UK

25 8 BP Exploration - Integrated Subsurface Description & Modelling, Bldg H, Desk W172  
26 Chertsey Road, Sunbury on Thames, TW16 7LN

27 9 University of Derby, Kedleston Road , Derby, DE22 1GB

28

## 29 **ABSTRACT**

30 Lacustrine carbonate deposits with spherulitic facies are poorly understood, but are key to  
31 understanding the economically important “Pre-Salt” Mesozoic strata of the South Atlantic.  
32 A major barrier to research into these unique and spectacular facies is the lack of good  
33 lacustrine spherulite-dominated deposits which are known in outcrop. Stratigraphy and  
34 petrography suggest one of the best analogue systems is found in the Carboniferous of  
35 Scotland: the East Kirkton Limestone. Here we propose a hydrogeochemical model that  
36 explains why the  $\text{CaCO}_3$ ,  $\text{SiO}_2$ , Mg-Si-Al mineral suite associated with spherular radial calcite  
37 facies forms in alkaline lakes above basaltic bedrock. Demonstrating links between igneous  
38 bedrock chemistry, lake and spring water chemistry and mineral precipitation, this model  
39 has implications for studies of lacustrine sediments in rift basins of all ages. Using empirical  
40 and theoretical approaches, we analyze the relationship between metal mobilization from  
41 sub-surface volcanoclastic rocks and the potential for precipitation of carbonate minerals,

various Mg-bearing minerals and chalcedony in a lacustrine spherulitic carbonate setting. This suite of minerals is most likely formed by in-gassing of CO<sub>2</sub> to a carbon-limited alkaline springwater, consistent with the reaction of alkali igneous rocks in the subsurface with meteoric groundwater. We suggest that an analogous system to that at East Kirkton caused development of the 'Pre-Salt' spherulitic carbonate deposits.

**Keywords:** Palaeozoic, magnesium silicate, calcite, hydrolysis, Pre-Salt, palaeogeography, lake, PHREEQC, Europe, Sediment mineralogy

## 1. INTRODUCTION

Fibro-radial spherulitic calcite components are relatively well known on a small scale from vadose, lacustrine and marine environments (Verrecchia et al., 1995; Braissant et al., 2003; Arp et al., 2012; Wanas, 2012; Casado et al., 2014; Bahniuk et al., 2015). However, deposits constituted of more than a few grains of spherulitic habit are rare, and probably limited to specific processes and depositional conditions that are currently poorly constrained. Comparatively little studied, there has been increasing interest in understanding how such voluminous lacustrine spherulitic calcite deposits, and the SiO<sub>2</sub> and Mg-Si-Al suite of minerals typically associated with them, were precipitated. This increased interest has been further motivated by the need to explain the economically-significant and spatially voluminous early Cretaceous 'Pre-Salt' carbonate reservoirs of Brazil and Angola (Wright, 2012; Wright and Barnett, 2015). The origin of these highly unusual deposits, which

occupied rift lakes formed during opening of the South Atlantic, is controversial (Wright, 2012; Mercedes-Martín et al., 2016). Crucial first-order questions, such as the source(s) of the calcium and silica being deposited, remain unanswered. The sheer masses of minerals precipitated from the Cretaceous lakes imply a major mass-transfer process operated at the time, but this process has not been identified. What is clear is that the petrographic appearances of these sediments is markedly different from known Recent “meteoene” or “tufa” carbonate deposits (Wright, 2012). Equally, the very high volume of carbonate emplaced demonstrates that these systems were not metal-limited as most modern “thermogene” or “travertine” deposits are (Guido and Campbell, 2011; Renaut et al., 2013). Such geologically unusual deposits imply an unusual mass transfer mechanism operated during rifting of the South Atlantic.

### **1.1. Fibro-Radial Calcite and the Great Pre-Salt Controversy**

In the ‘Pre-Salt’ South Atlantic rift lake rocks, fibro-radial carbonate components ‘float’ within Mg-rich clay deposits (Dias, 1998; Terra et al., 2010; Wright and Barnett, 2015). The precise genetic relationship between these Mg-Si and CaCO<sub>3</sub> phases is a subject of ongoing controversy that needs resolving if the origin of the ‘Pre-Salt’ deposits is to be elucidated (Mercedes-Martín et al., 2016). Hypotheses based on petrographic observations variously suggest fibro-radial calcite arises from displacive concretionary crystal growth within Mg-Si matrices (Dorobek et al., 2012), or as early diagenetic features from Mg-Si gel catalysis (Wright and Barnett, 2015) or as a consequence of crystal growth in the presence of specific organic compounds (Mercedes-Martin et al, 2016). All three hypotheses are yet to be

rigorously experimentally tested, and a major barrier to effective testing is a lack of suitable deposits that can be investigated beyond proprietary and confidential drill core material of the South Atlantic rift lakes. Some partial analogues are known from the literature, for example minor spherulitic facies are reported from the distal facies of Jurassic hot spring systems from Deseado Massif, Argentina (Guido and Campbell, 2011). Here we focus on the mechanisms leading to the precipitation of carbonates and silicates in a lacustrine Carboniferous analogue from Scotland, UK.

## **1.2. The East Kirkton Limestone: an interesting case study of rifting-related spherulitic limestones**

The Carboniferous East Kirkton Limestone of the Midland Valley graben of Scotland (Fig. 1) contains calcium carbonate spherulites, spherulitic bioherms, calcite-smectite laminites and primary chert (Rolfe et al., 1993; Walkden et al, 1993). It occurs as a Member of the upper part of the West Lothian Oil Shale Formation (Smith et al., 1993), and its petrology, paleontology, stratigraphy and isotope geochemistry were well described in studies from the 1980s and 1990s (Wood et al., 1985, McGill, 1994; McGill et al, 1994; Clarkson et al, 1993; Rolfe et al., 1993; Walkden et al., 1993; Goodacre, 1999). However, despite this significant effort to understand the East Kirkton Limestone, aspects of the system could not be elucidated two decades ago. A pivotal question lies in unravelling the source of the calcium and silica mass deposited in the lake, which is implicit in ongoing debates over whether the water in the lake was affected by deep-sourced “geothermal” springs (McGill et al., 1994).

107

108 The West Lothian Oil-Shale was deposited during a phase of rapid extension of the Midland  
109 Valley Basin, and these strata were strongly affected during their deposition by right lateral  
110 strike-slip movement which created half-grabens with tilted blocks forming inter-basin highs  
111 (Whyte, 1993; Read et al., 2002). Rift evolution was pulsed, with each phase of activity  
112 producing voluminous calc-alkaline extrusive igneous products (Monaghan and Parrish,  
113 2006). These products were interbedded as volcanoclastic rocks below, within and above the  
114 East Kirkton Limestone, indicating that the lacustrine phase was short-lived and coincided  
115 with an active volcanic pulse.

116 Basins opened throughout the South Atlantic in the Mesozoic from the Berriasian, due to  
117 rifting followed by strong thermal subsidence (Karner et al., 2003). In the southern basins of  
118 interest to this study (Moulin et al., 2005), rifting was active from the Barremian to base  
119 Aptian (Chaboureaud et al., 2013). The active rifting was characterised by widespread, largely  
120 trachytic, volcanism (Teboul et al., 2017) which was particularly voluminous in the southern  
121 sector, encompassing the Santos / Campo and South Kwanza basins (Chaboureaud et al.,  
122 2013). The Pre Salt carbonate formations developed during Early Aptian as accommodation  
123 was created by thermal sag of these rift basins (Karner et al., 2003). Volcanism continued  
124 within the Santos (Moreira et al., 2007) and Campos (Rangel et al., 1994) basins into the  
125 Aptian, reflecting that some lithospheric stretching continued into the period of extensive  
126 carbonate deposition. As at East Kirkton, lacustrine carbonate formations are therefore  
127 underlain by thick calc-alkaline volcanic materials, and deposition is associated within minor  
128 ongoing extrusive volcanic activity.

Overall, the East Kirkton Limestone seems an exceptional case study to better understand the origin of the mineral phases developed in rift volcanic lake settings such as those forming the South Atlantic 'Pre-Salt' deposits (sensu Dias, 1998, and Terra et al., 2010). The East Kirkton Limestone is also an important geoheritage site in its own right, famous for being the place where the earliest known well-preserved amphibian reptile skeleton was discovered (*Westlothiana lizziae*; Wood et al., 1985), so our findings have inherent value in further constraining a globally important early reptilian habitat.

## 2. MATERIALS AND METHODS

The type section of the East Kirkton Limestone is a quarry face (Fig. 1), where a heavily silicified spring emergence zone occurs at the northern limit giving way to layered carbonate, chalcedony and volcanoclastic deposits on its southern edge. This deposit was logged and sampled in August 2014. In addition, a series of boreholes (BH1, BH2 and BH3) drilled during 1987 and 1988 from the immediate area around the quarry were accessed, logged and sampled via the BGS Core Repository at Keyworth (UK) in February 2015. In particular, borehole BH2 is comprised of thick altered volcanoclastics attributed to unit 61 of the East Kirkton Limestone (see Rolfe et al., 1993), and borehole BH3 hosts more than 60 cm-thick tuffaceous rocks. Geochemical analyses were performed from samples in borehole BH3.

### 2.1. Optical and Energy-Dispersive X-Ray Spectroscopy (EDS) analysis

Optical microscopic examinations of thin sections were made with a Nikon Microphot FX microscope interfaced with a Nikon DS-Fi2 camera, and Nikon Elements D software. An



Oxford Instruments Peltier-cooled type X-Max 80 EDS system integrated with a Zeiss EVO60 Scanning Electron Microscopy was used to determine the abundance of specific elements through the X-rays energy spectrum. Rasterization of particular areas within the sample was implemented to obtain the chemical abundance of elements and create from matrix points, using a standard method within the INCA Energy software.

## **2.2. X-ray powder diffraction**

X-ray powder diffraction data were collected from ground samples mounted in stainless steel sample holders. A PANALYTICAL EMPYREAN diffractometer operating in Bragg-Brentano geometry with copper  $K\alpha_1$  ( $\lambda = 1.540546 \text{ \AA}$ ) and a PIXEL detector was used for the data collection.

## **2.3. Sr Isotopes**

The mobile fraction of strontium (i.e.  $\text{HNO}_3$  soluble) from samples taken from within the East Kirkton Limestone and from the altered igneous rocks of BH1 (Table 1) were extracted from powdered samples in PFA Teflon (Savillex) beakers on a hotplate at 140-150°C using ultrapure  $\text{HNO}_3$ . Analysis follows standard procedures (Henderson et al., 1994; Pin et al., 1994) with multiple  $\text{HNO}_3$  elutions from a Triskem Sr-spec resin packed Bio-Rad glass column. Pure strontium concentrates were loaded on to Re filaments using Ta emitter solution and analyses carried out on a VG sector 54-30 thermal ionisation Mass spectrometer at SUERC.

## **2.4. Organic Geochemistry**

Lipid biomarkers were extracted from c.2.8 – 4.0g of freeze-dried and homogenised sample, following the microwave-assisted extraction methodology of Kornilova and Rosell-Melé

(2003). Known concentrations of 5 $\alpha$ -cholestane and hexatriacontane (Sigma-Aldrich) were added as internal standards. Each total lipid extract was hydrolysed using 8% KOH in methanol, heated for 1 hr at 70°C and left overnight. Neutral fractions were recovered using repeated liquid extraction with hexane, then separated into apolar, ketone and polar fractions using silica column chromatography and *n*-hexane, dichloromethane and methanol as eluents, respectively. The apolar fractions were analysed by gas chromatography-mass spectrometry (GC-MS), using a 30m HP-5MS fused silica column (0.25 mm i.d. 0.25 $\mu$ m of 5% phenyl methyl siloxane). The carrier gas was He, and the oven temperature was programmed as follows: 60-200°C at 20°C/min, then to 320°C (held 35 min) at 6°C/min. The mass spectrometer was operated in full-scan mode (50-650 amu/s, electron voltage 70eV, source temperature 230°C). Quantification was achieved through comparison of integrated peak areas in the total ion chromatograms and those of the internal standards.

Known concentrations of 5 $\alpha$ -cholestane and hexatriacontane (Sigma-Aldrich) were added as internal standards. Each lipid extract was hydrolysed using 8% KOH in methanol, heated for 1 hr at 70°C and left overnight. Neutral fractions were recovered using repeated liquid extraction with hexane, then separated into apolar, ketone and polar fractions using silica column chromatography and *n*-hexane, dichloromethane and methanol as eluents, respectively. The apolar fractions were analysed by gas chromatography-mass spectrometry (GC-MS), using a 30m HP-5MS fused silica column (0.25 mm i.d. 0.25 $\mu$ m of 5% phenyl methyl siloxane). The carrier gas was He, and the oven temperature was programmed as follows: 60-200°C at 20°C/min, then to 320°C (held 35 min) at 6°C/min. The mass spectrometer was operated in full-scan mode (50-650 amu/s, electron voltage 70eV, source

temperature 230°C). Quantification was achieved through comparison of integrated peak areas in the total ion chromatograms and those of the internal standards.

### 3. RESULTS

The general stratigraphy, mineralogy and geochemistry of the East Kirkton Limestone were previously described by Clarkson et al., 1993; Rolfe et al., 1993; Smith et al., 1993; Walkden et al., 1993; McGill et al, 1994; Goodacre, 1998. The most significant facies (Fig. 2, Fig. S1) and a representative sedimentary facies log (borehole BH3, Fig. 3) are provided to illustrate the main stratigraphic features. The mineral assemblages and stratigraphic context of these deposits are comparable to those documented so far in the South Atlantic 'Pre-Salt' rift lakes (*sensu* Bertani and Carozzi, 1985; Dias, 1998; Terra et al., 2010; Tosca and Wright, 2015; Saller et al., 2016). We make this claim on the basis of: i) the occurrence of meter-scale beds yielding abundant partially eroded fibro-radial, spherical calcite components about 1mm in size and displaying sweeping extinction; ii) the presence of serpentine-rich floatstone of spherulitic components; iii) the laminated nature of the alternations of Mg-Si and CaCO<sub>3</sub> mineral phases throughout; and the presence of significant chalcedony and calcite cementing both Mg-Si and Ca phases (Fig. 4), iv) presence of mature hydrocarbons stored in spherulitic biohermal reservoir facies (Fig. S1F).

Thin section and XRD analyses (Figs. 4 and 5) both demonstrate that the primary carbonate mineralogy is dominantly calcite, with silica and dolomite as secondary phases: the composition and mineral paragenesis of this rock is consistent with currently published data

on South Atlantic 'Pre-Salt' deposits (Bertani and Carozzi, 1985; Dias, 1998; Terra et al., 2010; Tosca and Wright, 2015; Saller et al., 2016). It is possibly coincidental that the East Kirkton Limestone contains abundant mature hydrocarbons (Fig. 6), which have likely migrated into this reservoir facies from the black lacustrine West Lothian Oil-shale, however this does illustrate that it occurs in a hydrocarbon-prone basin context analogous to the Pre Salt and that migration of mature hydrocarbons and their formation waters are shared features of the paragenesis of both deposits.

### **3.1. Stratigraphic relationships**

Borehole BH-3 (Fig. 3) displays a soil and rock cover in the first 3 m. Spherulitic carbonates are found between 2.8 and 3.6 m and between 4.3 and 6.2 m depth occurring as laminites, which are formed by the alternation of carbonate-rich and organic-rich laminae hosting abundant calcite spherulitic components (Fig. 2B, C; Fig. S1A, B). In some cases, a large number of spherulites are found floating in clay/organic to mudstone-rich matrices producing floatstone textures (Fig. 2D). Soft-sediment deformation (slumps, creeping of laminae, Fig. 2A, Fig. S1B) and diverse biota is occasionally recognised in laminites (Fig. S1C). Some cm-scale calcareous-rich tuff layers are interbedded within the sequence (from 3.6 to 3.8m depth, Fig. S1D) which hardly ever contains spherulitic components. Three organic-rich shale packages (3.8 to 4.3 m; 6.2 to 7.3 m, and 7.8 to 13.5 m depth) previously named Little Cliff Shale Member by Rolfe et al., (1993) are also recorded. These authors identified pelecypods (*Curvirimula scotica*), plants (*Lepidodendron*), fish scales, ostracods (*Carbonita*),

and arthropods. A 50cm-thick layered carbonate interval (Fig. 3A) is recorded between 7.3 and 7.8 m depths displaying nodular to tabular beds of wackestone to floatstone textures. Evidence of slumps and convolute beds is present and peloids, fish scales and ostracods allochems are common. In the bottom of the borehole (between 13.5 and 14.6 m depth) a greenish to dark orange tuff is recognised (Fig. 3, Fig. S1D). This unit is characterised by a pyroclastic texture with mm-thick angular to subangular lapilli clasts surrounded by fine-grained vesicular and amygdaloidal ash and shards (Fig. S1D). In some cases, calcite pseudomorphs after altered amygdale textures were observed emplaced within plagioclase or olivine phenocrysts (Fig. 2E), and some of these alkali minerals showed alteration textures to serpentine-like clay minerals. In addition, centimetre-sized irregular cavities filled with sequential generations of fibroradial/spherulitic chalcedony and drusy megaquartz cements (Fig. 2F) are also present in some spherulitic biohermal carbonate units (not shown in the log, Fig. S1F)..

### **3.2. Petrological observations**

XRD analyses of the tuffs underlying the East Kirkton section indicate they have now completely replaced to calcite (Fig. 5A). The spatially-resolved EDS map of the altered tuff (across the white square in Fig. 5A) shows that pure calcite cement occurs as a light coloured fabric under plane-polarized light (top left in Fig. 3A, corresponding to high concentrations of Ca in Fig. 5B). A greenish brown area rich in Al, Mg and Fe (center and top-right in Fig. 5A, corresponding to high concentrations of these elements in Fig. 5B) is a

serpentine-like clay alteration product (Fig. 5C), similar to that encountered in the lacustrine deposits located higher in the East Kirkton stratigraphy (Fig. 5). A pale green region in the bottom left (Fig. 5A) is rich in K and Al and likely contains un-altered components of the original feldspar mineral phase.

### **3.3. Strontium isotope data**

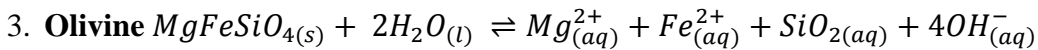
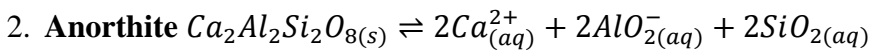
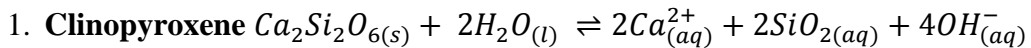
Results of strontium isotope analysis (Fig. 7) demonstrate that a substantial component of this metal was ultimately derived from a mantle source. Also, comparison with the BH3 material and published data for the Midland Valley volcanic rocks indicate that BH3 volcanic tuffs and the lacustrine carbonate deposit are geochemically compatible, and probably co-developed, whereas both are less radiogenic than the original volcanic rocks.

## **4. DISCUSSION**

Overall, the tectono-stratigraphic context and mineral paragenesis recognised at East Kirkton are compellingly similar to the Pre-Salt deposits, representing a unique opportunity to study the hydrogeochemical processes enabling the development of these unusual deposits in detail. As with Pre Salt deposits, we interpret the East Kirkton deposit as an alkaline lake fed by springs with a high dissolved mass. Interpretation that the East Kirkton Limestone formed in an alkaline lake fed by a hot-spring are not new (McGill et al., 1993; Walkden et al., 1993). However, no previous study has been able to deduce the origin of the carbonate and silica-rich solutions contributing to the lake water mass. Here we present new petrographical analyses showing that the tuff in borehole BH3 underlying the

Limestone deposit (Fig. 3, Fig. 5, and S1D) displays textural and chemical evidence of replacement and alteration (Fig. 2E, 5) and only a faint geochemical signature of the original mineralogy can be identified. This alteration moved the  $^{87}\text{Sr}/^{86}\text{Sr}$  ratio away from the composition of unaltered regional igneous rocks, towards a composition also seen in the spherulitic carbonate deposits vertically above (Fig. 7). We infer that these two systems were in connection, and that the altering water was derived from meteoric input (Walkden et al., 1993).

The composition of Midland Valley Carboniferous extrusive igneous rocks nearby (Monaghan and Parrish, 2006) indicate that the original mineralogy of this material was a fairly standard pyroxene-olivine-feldspar assemblage, and this is compatible with the remnant Mg, Fe, K, Al found within the weathered tuffs (Fig. 5). The dominance of Ca in the weathered residue indicates that the feldspars were close to the anorthite end member and the pyroxenes were close to the Ca-rich end member in the original mineralogy. These minerals are known to be prone to weathering by infiltrating water, and undergo the following hydrolysis reactions (Equations 1-3), which are essentially the metasomatic reactions involved in serpentinization (Müntener, 2010; Hövelmann et al., 2011).



In all three reactions, the dissolved products cause hydrolysis resulting in very alkaline solutions. Ultimately, the solution produced by these reactions: i) will have a very high pH; ii) will be reducing; iii) will be rich in Ca, Si, Al, Mg and Fe. The molar ratios of fluid reaching the Earth's surface will be determined by 1) the molar ratios in the original rock, and 2) the molar ratio of secondary precipitates left by the solution in the subsurface.

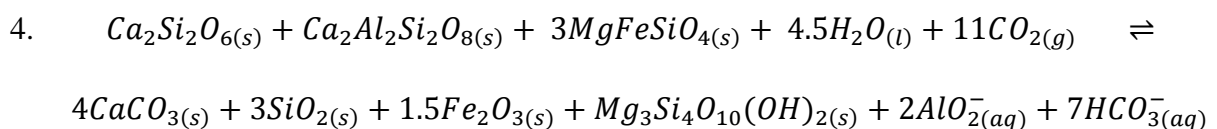
The abundance of carbonate secondary precipitates in BH1 (Fig. 5) shows that the precipitating fluid contained substantial amounts of dissolved inorganic carbon. This is common in both meteogene and thermogene settings (Pentecost, 2005), and results in significant deposition of carbonate minerals as observed in this case. Consequently, although the Midland Valley volcanic series can be expected to have contained >10% calcium by mass, springs reaching the surface having altered these rocks will be severely calcium-limited. This is observed in modern springs, even where pH has been raised above 10 by reactions analogous to equations 1-3 (Jones and Renaut, 2010; Renaut et al., 2013). To explain the Ca-rich spring implied by the spherulitic nature of the deposits at East Kirkton (Wright and Barnett, 2015; Mercedes-Martín et al., 2016), and more dramatically the exceptionally large mass of calcium deposited within the Pre-Salt Formations (Dias, 1998; Terra et al., 2010), such calcium limitation cannot have occurred, and the amount of calcium available to the subsurface fluids must have exceeded the capacity of the dissolved carbon supply to remove it. This implies that the waters were not geothermally sourced but were meteoric, and that the whole East Kirkton system was consuming very large masses of carbon derived from the atmosphere. Large-scale geochemical systems fulfilling this



description occur today within exhumed ophiolites, for example the Somail Ophiolite in Oman (Matter and Kelemen, 2009). Springs fed from carbon-limited reactions in the subsurface have led to the deposition of an estimated  $10^7$  m<sup>3</sup> of carbonate on the surface, covering an area of ~200,000 m<sup>2</sup>, in the last ~50,000 years alone (Kelemen and Matter, 2008). We propose that an analogous geochemical system led to the development of both the East Kirkton and Pre-Salt carbonate formations.

#### 4.1. Understanding a Carbon-Limited, Hyperalkaline Spring System

On emergence at the surface, a carbon-limited solution produced by weathering alkaline tuff would rapidly equilibrate by reacting with atmospheric CO<sub>2(g)</sub> to produce a range of mineral products. Summatively, reactions 1-3 and 4 result in a balanced transfer of mass from clinopyroxene, olivine and feldspar to calcite, silica and serpentine-like clay (stevensite at high pH and high Mg/ Si ratios; Tosca and Masterton, 2014) and Mg-Al phases, and these reactions are essentially identical to those reported from weathering ophiolite systems (Kelemen and Matter, 2008).



Our hypothesis is that there is no geothermal heating from active magma systems from which excess CO<sub>2</sub> could be provided, however this does not imply the spring was necessarily cold. Reactions 1-4 are exothermic (Wenner and Taylor, 1971), so it is likely the waters

arising from them were warm. Temperatures as high as 60°C for the East Kirkton lake water have been inferred from  $\delta^{18}\text{O}$  in silica (McGill et al, 1993). We note that Walkden et al. (1993) estimated an average lake temperature of 20°C from oxygen isotopes in calcite spherules, however this facies may reflect a distal setting in which significant dissolved organic matter was present in solution (Mercedes-Martin et al., 2016) as reported in Patagonia (Guido and Campbell, 2011). The high-temperature siliceous facies and the low-temperature spherulite facies are therefore compatible with relatively high (proximal) and low (distal) spring influence respectively. In any case, the importance of identifying whether the water was hot or cold derives, in large part, from the value of raised temperature as a proxy for a non-karstic source for the calcium and carbonate ions. Our analysis indicates that these ions were sourced from igneous rock weathering regardless of spring water temperature, and so the emphasis on understanding temperature is much reduced.

The evolution of the solution, and the paragenesis of depositional products derived from it, can be explored by sequentially exposing a spring representative of carbon-limited reactions 1-3 to  $\text{CO}_{2(\text{g})}$  at surface conditions using a simple thermodynamic approach via PHREEQC modelling (Parkhurst and Appelo, 1999; Fig. 8, See Supplementary Material). Here, we use a representative springwater from the Somail Ophiolite (see Supplementary material). We find that Mg-Si phases are most insoluble initially;  $\text{CaCO}_3$  phases precipitate in almost stoichiometric balance with the ingassing of carbon dioxide; and  $\text{SiO}_2$  phases increase in insolubility as pH falls (Fig. 8). Indeed, by allowing the system to achieve equilibrium with excess  $\text{CO}_2$ , we can also investigate the predicted paragenesis for the mineral assemblage.

Figure 4 shows that with increasing ingassing, serpentine-like Mg-Si phases remineralize to a combination of Mg-Al phases and dolomite as  $\text{OH}^-_{(\text{aq})}$  becomes unavailable below the pH  $\sim 10$  transition, which is consistent with paragenesis concepts for the Pre-Salt (Wright and Barnett, 2015). Simultaneous deposition of calcite, silica, dolomite and serpentine-like clays around the lake shores implies an equilibrium pH of  $\sim 8$  for lake waters (Fig. 8), comfortably within the range of modern alkaline surface waters (Rogerson et al., 2014). Alternation of calcite- and silica-dominated phases in the more distal lake environments in this case is consistent with an oscillation of water chemistry around pH 7, presumably reflecting variable balance in the input flux of spring and ambient meteoric water. However, this result is unlikely to be unique and may reflect the specific chemistry of the spring system itself. The diagenetic changes implied by the succession of Mg-phases in Figure 8 indicate that secondary porosity is likely to develop. This is consistent with the behaviour of Mg-Si in the Pre-Salt system as more fully developed by Tosca and Wright (2015).

#### **4.2. Is Carbon-limited Mass Transfer to Terrestrial Carbonates a Significant Sediment Transport Process?**

The similarity of the sediments and mineral phases at East Kirkton to those of the larger South Atlantic Cretaceous lakes implies a strong similarity in their genetic processes, and therefore that similar mass-transfer geochemical processes are likely to have been operating on a very large scale in the early Mesozoic. Indeed, the geochemical signature of subsurface alteration of this type has also been reported for the igneous series underlying the 'Pre-Salt' carbonates. During rainy periods chemical weathering of basic volcanoclastic

390 rocks and basaltic magmas is thought to have promoted an active transport of dissolved  
391 cations (Na, Ca, K, Mg) into the Lagoa Feia lake ('Pre-Salt', Brazil; Bertani and Carozzi, 1985).  
392 In addition, extensive calcitization processes and trioctahedral smectite formation took  
393 place in the distal parts of the lacustrine terrigenous flats (Bertani and Carozzi, 1985).  
394 Serpentinization of the exhumed mantle in several Brazilian 'Pre-Salt' basins can have  
395 occurred down to depths of 6-8 km at the continental-oceanic crustal transition (Zalán et al.,  
396 2011), providing an enormous reservoir of dissolved cations from igneous source rocks for  
397 remobilisation in the 'Pre-Salt' lakes. Recent re-evaluation of the igneous series underlying  
398 the Kwanza Pre-Salt basin offshore of Angola again indicates meteoric alteration, and  
399 development of metal-rich fluids (Teboul et al., 2017). Our hypothesis only requires that this  
400 alteration is done by relatively carbon-poor meteoric waters so that subsurface reactions  
401 were carbon-limited not calcium-limited. In the case of the Kwanza basin, this is consistent  
402 with low temperature alteration yielding highly alkaline, Mg, Ca and Si-rich solutions and  
403 may have occurred early during alteration (Teboul et al., 2017). Later fluids, and thus  
404 equilibrium mineral phases in the altered igneous rocks, indicate high-temperature  
405 alteration from fluids rich in CO<sub>2</sub> (Teboul et al., 2017).  
406 The primary difference between the East Kirkton deposit (spatial scale ~100's m) and Pre  
407 Salt systems (~100s km) is scale, and some care is needed before mass transfer processes  
408 can be assumed to apply over 3 orders of magnitude. However, as the scale of the lake  
409 system being considered increases the potential to capture increasing numbers of large  
410 spring systems also increases. It is clearly impossible that a Pre Salt system could be fed by a  
411 single point source, as appears to be the case in East Kirkton. However, we see no reason

why multiple sources cannot be sufficient to condition a large lake watercolumn chemistry just as a single source conditions a small one. The primary difference will be multiple, potentially independently evolving, points of calcium, magnesium and silica supply to the lake to be active, likely giving rise to complex spatial and temporal variability in sedimentary facies and early diagenesis.

If this hypothesis is correct, the subsurface mass-transfer through pumping of aqueous solutions described at East Kirkton is capable of acting over scales of hundreds of kilometres. This is a basin-scale sedimentary process that has received very scant investigation, but may be repeated and predictable in basins where rapid extension and volcanic exhumation is taking place with dominantly low-lying, terrestrial conditions at the surface. We propose the East Kirkton Limestone as a type system for further investigation of this new carbon-limited mass transfer and depositional systems associated with subsurface alkaline rock weathering.

## **5. CONCLUSIONS**

We hypothesise that the East Kirkton Limestone is the depositional end of a little recognised mass-transfer process originating with subsurface geochemical alteration of alkaline igneous volcanic rocks, acting through carbon-limited spring systems, which may have been heated by the reactions themselves, and terminating in potentially basin-scale lacustrine deposition in which minerals are formed from the mixture of spring water and atmospheric carbon. Today, this process occurs within exhumed ophiolites but may also be associated with a specific phase during crustal extension. The East Kirkton lithofacies and mineral assemblages

(carbonates, Mg-Si phases, and chalcedony) are so analogous to, and the geological background so coherent with, the South Atlantic Cretaceous 'Pre-Salt' strata that we conclude that similar processes are likely to have been acting there. Understanding the mass-transfer dynamics of hydrochemical systems in the subsurface will be fundamental to a process-based understanding of the origin of the spherical-radial carbonate phases recorded both at East Kirkton and in the 'Pre-Salt' deposits, and forms an intriguing new perspective on both the fate of metal mass remobilisation from extrusive igneous processes in these contexts and the geothermal significance of alkaline warm and hot springs.

#### **ACKNOWLEDGEMENTS**

BP Exploration Co. is thanked for funding, and particularly the Carbonate Team for supporting this research and for fruitful discussions. West Lothian Council and Scottish Natural Heritage are thanked for allowing access and permission for sampling the site. The Core Store Team at BGS Keyworth is particularly acknowledged for their assistance. Mark Anderson, Tony Sinclair (University of Hull), and Bouk Lacet (VU University Amsterdam) are thanked for technical support. Anne Kelly (SUERC) for carrying out the Strontium Isotope analyses. Mark Tyrer is thanked for his advice on PHREEQC modelling.

#### **REFERENCES CITED**

Arp, G., Helms, G., Karlinska, K., Schumann, G., Reimer, A., Reitner, J., and Trichet, J., 2012, Photosynthesis versus exopolymer degradation in the formation of microbialites on the

atoll of Kiritimati, Republic of Kiribati, Central Pacific: *Geomicrobiology Journal*, v. 29, no. 1, p. 29-65.

Bahniuk, A.M., Anjos, S., França, A. B., Matsuda, N., Eiler, J., McKenzie, J. A., and Vasconcelos, C., 2015, Development of microbial carbonates in the Lower Cretaceous Codó Formation (north-east Brazil): Implications for interpretation of microbialite facies associations and palaeoenvironmental conditions: *Sedimentology*, v. 62, no. 1, p. 155-181.

Bertani, R.T., and Carozzi, A.V., 1985. Lagoa Feia Formation (Lower Cretaceous) Campos Basin, offshore Brazil: rift valley type lacustrine carbonate reservoirs – II: *Journal of Petroleum Geology*, v. 8, no. 2, p. 199-220.

Braissant, O., Cailleau, G., Dupraz, C., and Verrecchia, E.P., 2003. Bacterially induced mineralization of calcium carbonate in terrestrial environments: the role of exopolysaccharides and amino acids: *Journal of Sedimentary Research*, v. 73, p. 485-490.

Cameron, I. B., Aitken, A. M., Browne, M. A. E., Sepsenon, D. (1998). *Geology of the Falkirk district: memoir for 1: 50 000 geological sheet 31E (Scotland)*. London, The Stationery Office. 106pp.

Casado, A.I., Alonso-Zarza, A. M., and La Iglesia, A., 2014. Morphology and origin of dolomite in paleosols and lacustrine sequences. Examples from the Miocene of the Madrid Basin: *Sedimentary Geology*, v. 312, p. 50-62.

Chaboreau, A.C., Guillocheau, F., Robin, C., Moulin, M., Aslanian, D., 2013. Paleogeographic evolution of the central segment of the South Atlantic during the Early Cretaceous times : paleotopographic and geodynamic implications. *Tectonophysics* 604, 191-223.

478 Clarkson, E.N.K., Milner, A.R., and Coates, M.I., 1993. Palaeoecology of the Viséan of East  
 479 Kirkton, West Lothian, Scotland: Transactions of the Royal Society of Edinburgh: Earth  
 480 Sciences, v. 84, p. 417-425.

481 Dewandel, B., Lachassagne, P., Boudier, F., Al-Hatali, S., Ladouche, B., Pinault, J.-L., Al-  
 482 Suleimani, Z., 2005. A conceptual model of ophiolite hard-rock aquifers in Oman based  
 483 on a multiscale and a multidisciplinary approach. Hydrogeology Journal 13, 708-726.

484 Dias, L.J., 1998, Análise sedimentológica e estratigráfica do Andar aptiano em parte da  
 485 margem leste do Brasil e no platô das Malvinas: considerações sobre as primeiras  
 486 incursões e ingressões marinhas do oceano Atlântico Sul Meridional [Ph.D. thesis]: Brazil,  
 487 Universidade Federal do Rio Grande do Sul, 411p.

488 Dorobek, S., Piccoli, L., Coffey, B. and Adams, A., 2012. Carbonate rock-forming processes in  
 489 the Presalt “sag” successions of Campos Basin, offshore Brazil: evidence for seasonal,  
 490 dominantly abiotic carbonate precipitation, substrate controls, and broader geologic  
 491 implications: AAPG Hedberg Conference “Microbial Carbonate Reservoir  
 492 Characterization” Abstracts. Houston Texas.

493 Goodacre, I.R., 1999. Microbial carbonates in lacustrine settings: an investigation into the  
 494 Carboniferous East Kirkton Limestone [Ph.D. thesis]: Scotland, University of Aberdeen,  
 495 253p.

496 Guido, D.M., Campbell, K.A., 2011. Jurassic hot spring deposits of the Deseado Massif  
 497 (Patagonia, Argentina): Characteristics and controls on regional distribution: Journal of  
 498 Volcanology and Geothermal Research, v.203, 35-47.



499 Henderson, G., Martel, D., O'Nions, R., Shackleton, N., 1994. Evolution of seawater  $^{87}\text{Sr}/^{86}\text{Sr}$   
 500 over the last 400 ka: the absence of glacial/interglacial cycles: *Earth and Planetary*  
 501 *Science Letters*, v.128, 643-651.

502 Hövelmann, J., Austrheim, H., Beinlich, A., and Anne Munz, A., 2011. Experimental study of  
 503 the carbonation of partially serpentinized and weathered peridotites: *Geochimica et*  
 504 *Cosmochimica Acta*, v.75, p. 6760-6779.

505 Jones, B., Renaut, R.W., 2010. Calcareous Spring Deposits in Continental Settings.  
 506 *Sedimentology*, v.61, 177-224.

507 Karner, G.D., Driscoll, N.W., Barker, D.H.N, 2003. Syn-rift region subsidence across the West  
 508 African continental margin; the role of lower plate ductile extension, In: Arthur, T.J.,  
 509 MacGregor, D.A.S., Cameron, N.R. (Eds.), *Geological Society of London, Special*  
 510 *Publications* 207, 105-129

511 Kelemen, P.B., Matter, J., 2008. In situ carbonation of peridotite for CO<sub>2</sub> storage.  
 512 *Proceedings of the National Academy of Sciences*, v.105, 17295-17300.

513 Matter, J.M., Kelemen, P.B., 2009. Permanent storage of carbon dioxide in geological  
 514 reservoirs by mineral carbonation. *Nature Geoscience*, v.2, 837-841.

515 McGill, R.A.R., 1994. Geochemistry and petrography of a Lower Carboniferous, lacustrine,  
 516 hot spring deposit: East Kirkton, Bathgate, Scotland [Ph.D. thesis]: Scotland, University of  
 517 Glasgow, 173p.

518 McGill, R.A.R., Hall, A.J., Fallick, A. E., and Boyce, A. J., 1994. The paleoenvironment of East  
 519 Kirkton, West Lothian, Scotland: stable isotope evidence from silicates and sulphides:  
 520 *Transactions-Royal Society of Edinburgh: Earth Sciences* v. 84, p. 223-237.

521 Mercedes-Martín, R., Rogerson, M., Brasier, A. T., Vonhof, H. B., Prior, T. J., Fellows, S. M.,  
 522 Reijmer, J.J.G., Billing, I., Pedley, H. M., 2016. Growing spherulitic grains in saline,  
 523 hyperalkaline lakes: experimental evaluation of the effects of Mg-clays and organic acids.  
 524 *Sedimentary Geology* v. 335, p. 93-102  
 525 Monaghan, A.A., and Parrish, R.R., 2006. Geochronology of Carboniferous-Permian  
 526 magmatism in the Midland Valley of Scotland: Implications for regional tectonomagmatic  
 527 evolution and the numerical time scale: *Journal of the Geological Society* v.163, p. 15-28.  
 528 Moreira, J.L.P., Madeira, C.V., Gil, J.A., Machado, M.A.P., 2007. Bacia de Santos. *Boletim de*  
 529 *Geosciencias da Petrobras* 15, 531-549.  
 530 Moulin, M., Aslanian, D., Olivet, J., Contrucci, I., Matias, L., Geli, L., Klingelhoefer, F., Nouze,  
 531 H., Rabineau, M., Labails, C., Rehault, J., Unternehr, P., 2005. Geological constraints on the  
 532 evolution of the Angolan margin based on reflection and refraction seismic data (ZaiAngo  
 533 Project). *Geophysical Journal International* 162, 793-810.  
 534 Müntener, O., 2010. Serpentine and serpentinization: a link between planet formation and  
 535 life: *Geological Society of America*, v. 38, no. 10, p. 959-960.  
 536 Palmer, M.R., Edmond, J.M., 1989. The Strontium Isotope Budget of the Modern Ocean.  
 537 *Earth and Planetary Science Letters* 92, 11-26.  
 538 Parkhurst, D.L., and Appelo, C A.J., 1999. User's guide to PHREEQC (Version 2): A computer  
 539 program for speciation, batch-reaction, one-dimensional transport, and inverse  
 540 geochemical calculations. 312 p.  
 541 Pentecost, A., 2005. *Travertine*. Springer, Berlin.

542 Pin, C., Briot, D., Bassin, C., Poitrasson, F., 1994. Concomitant separation of strontium and  
 543 samarium-neodymium for isotopic analysis in silicate samples, based on specific  
 544 extraction chromatography. *Analytica Chimica Acta* v. 298, 209-217.

545 Rangel, H.D., Martins, F.A.L, Esteves, F.R., Feijo, F.J., 1994. Bacia de Campos. *Boletim de*  
 546 *Geosciencias da Petrobras* 8, 203-217.

547 Read, W.A., Browne, M.A.E., Stephenson, and D. Upton, B.J.G., 2002. Carboniferous, *in*  
 548 Trewin, N. H., ed., *The Geology of Scotland*, 4th. Geological Society, London, p. 251–300.

549 Renaut, R.W., Owen, R.B., Jones, B., Tercelin, J.J., Tarits, C., Ego, J.K., Konhauser, K.O., 2013.  
 550 Impact of lake-level changes on the formation of thermogene travertine in continental  
 551 rifts: Evidence from Lake Bogoria, Kenya Rift Valley. *Sedimentology*, v.60, 428-468.

552 Rogerson, M., Pedley, M., Kelham, A. and Wadhawan, J., 2014, Linking mineralisation  
 553 process and sedimentary product in terrestrial carbonates using a solution thermodynamic  
 554 approach: *Earth Surface Dynamics* v. 2, p. 197-216.

555 Rolfe, W.D.I., Durant, G.P, Baird, W. J., Chaplin, C, Paton, R. L., and Reekie, R. J., 1993, The  
 556 East Kirkton Limestone, Viséan, of West Lothian, Scotland: introduction and stratigraphy:  
 557 *Transactions of the Royal Society of Edinburgh: Earth Sciences*, v. 84, no. 3-4, p. 177-188.

558 Saller, A., Rushton, S., Buambua, L., Inman, K., McNeil, R., & Dickson, J.T., 2016. Presalt  
 559 stratigraphy and depositional systems in the Kwanza Basin, offshore Angola. *AAPG*  
 560 *Bulletin*, 100(7), 1135-1164.

561 Smith, R.A., Stephenson, D. and Monro, S.K., 1993. The geological setting of the southern  
 562 Bathgate hills, West Lothian, Scotland: *Transactions of the Royal Society of Edinburgh:*  
 563 *Earth Sciences*, v. 4, no. 3-4, p.189-196.

564 Smedley, P.L., 1986. The relationship between calc-alkaline volcanism and within-plate  
565 continental rift volcanism: evidence from Scottish Palaeozoic lavas. *Earth and Planetary*  
566 *Science Letters* 77, 113-128.

567 Stanger, G., 1986. The hydrogeology of the Oman Mountains. Open University.

568 Teboul, P.-A., Kluska, J.-M., Marty, N.C.M., Debure, M., Durlet, C., Virgone, A., Gaucher, E.C.,  
569 2017. Volcanic rock alterations of the Kwanza Basin, offshore Angola - Insights from an  
570 integrated petrological, geochemical and numerical approach. *Marine and Petroleum*  
571 *Geology* 80, 394-411.

572 Terra, G.J.S., Spadini, A.R., França, A.B., Sombra, C.L., Zambonato, E.E., Juschaks, L.C.d.S.,  
573 Arienti, L.M., Erthal, M.M., Blauth, M., Franco, P.P., Matsuda, N.S., da Silva, N.G.C.,  
574 Junior, P.A.M., D'Avila, R.S.F., deSouza, R.S., Tonietto, S.N., dos Anjos, S.M.C., Campinho,  
575 V.S. and Winter, W.R., 2010, Classificação de rochas carbonáticas aplicável às bacias  
576 sedimentares brasileiras: Bulletin Geoscience Petrobras, Rio de Janeiro, v.18, p. 9-29.

577 Tosca, N.J., and Wright, V.P., 2015. Diagenetic pathways linked to labile Mg-clays in  
578 lacustrine carbonate reservoirs: a model for the origin of secondary porosity in the  
579 Cretaceous pre-salt Barra Velha Formation, offshore Brazil, *in* Armitage, P. J., Butcher, A.  
580 R., Churchill, J. M., Csoma, A. E., Hollis, C., Lander, R. H., Omma, J. E., and Worden, R. H.,  
581 eds., *Reservoir quality of clastic and carbonate rocks: analysis, modelling and prediction:*  
582 Geological Society, London, Special Publications, 435, SP435-1.

583 Veizer, J., Ala, D., Azmy, K., Bruckschen, P., Buhl, D., Bruhn, F., Carden, G.A.F., Diener, A.,  
584 Ebner, S., Goddérès, Y., Jasper, T., Korte, C., Pawellek, F., Podlaha, O.G., Strauss, H.,

585 1999.  $^{87}\text{Sr}/^{86}\text{Sr}$ ,  $^{13}\text{C}$  and  $^{18}\text{O}$  evolution of Phanerozoic seawater. *Chemical Geology* 161,  
 586 59-88.

587 Verrecchia, E. P., Freytet, P., Verrecchia, K. E., and Dumont, J-L., 1995, Spherulites in calcrete  
 588 laminar crusts: biogenic  $\text{Ca CO}_3$  precipitation as a major contributor to crust formation:  
 589 *Journal of Sedimentary Research*, v. 65A, no. 4, p. 690-700.

590 Walkden, G. M., Roddy Irwin, J., and Fallick, A. E., 1993, Carbonate spherules and botryoids  
 591 as lake floor cements in the East Kirkton Limestone of West Lothian, Scotland:  
 592 *Transactions of the Royal Society of Edinburgh: Earth Sciences*, v. 84, no. 3-4, p. 213-221.

593 Wanas, H. A., 2012. Pseudospherulitic fibrous calcite from the Quaternary shallow lacustrine  
 594 carbonates of the Farafra Oasis, Western Desert, Egypt: A primary precipitate with  
 595 possible bacterial influence: *Journal of African Earth Sciences*, v. 65, p. 105–114.

596 Wenner, D.B., and Taylor, H.P., 1971. Temperatures of serpentinization of ultramafic rocks  
 597 based on  $\text{O}^{18}/\text{O}^{16}$  fractionation between coexisting serpentine and magnetite:  
 598 *Contributions to Mineralogy and Petrology*, v. 32, no. 3, p.165-185.

599 Whyte, M. A., 1993. Scottish Carboniferous fresh-water limestones in their regional setting:  
 600 *Transactions of the Royal Society of Edinburgh: Earth Sciences*, v. 84, no.3-4, p. 239-248

601 Wood, S. P., Panchen, A. L. and Smithson, T. R., 1985. A terrestrial fauna from the Scottish  
 602 Lower Carboniferous: *Nature*, v. 314, p. 355-356.

603 Wright, V. P., 2012. Lacustrine carbonates in rift settings: the interaction of volcanic and  
 604 microbial processes on carbonate deposition, *in* Garland, L. E. Neilson, S. E., Laubach, and

Whidden, K. J., eds. *Advances in carbonate exploration and reservoir analysis: Geological Society, London, Special Publications 370*, p. 39-47.

Wright, V. P., Barnett, A. J., 2015, An abiotic model for the development of textures in some South Atlantic early Cretaceous lacustrine carbonates, *in* Bosence, D. W. J., Gibbons, K. A., le Heron, D. P., Morgan, W. A., Pritchard, T. and Vining, B. A., eds. *Microbial Carbonates in Space and Time: Implications for Global Exploration and Production: Geological Society, London, Special Publications 418*, p. 209-219.

Zalán, P.V., Severino, M.D.C.G., Rigoti, C.A., Magnavita, L.P., and Bach, J.A., 2011. An entirely new 3D-view of the crustal and mantle structure of a South Atlantic passive margin-Santos, Campos and Espírito Santo basins, Brazil. AAPG, Annual Convention and Exhibition, Houston, Abstracts, p. 12.

## FIGURE CAPTIONS

**Figure 1.** Geological setting of the East Kirkton Limestone Quarry (red square). Limestones occur interbedded within coeval tuffs and basalt lavas. Location of the studied borehole BH-3 in the study area (modified from Cameron et al, 1998).

**Figure 2..** Main facies types. A) Spherulitic carbonates affected by different scales of soft-sediment deformation. Hammer for scale. B) Spherulitic components are embedded in organic-rich muddy matrices displaying floatstone to laminite textures. C) Spherulites are

composed of fibro-radial calcite generating spherical or elongated particles seen in crossed Nichols. EDS analysis on carbonate spherulites confirms calcite mineralogy (Cc: calcite, Mgc: low-magnesium calcite). D) Floatstone of volcanic remains (Volc) and spherulites (Spher) in a serpentine-like amorphous matrix (Am. silicate). Calcite cements crosscut previous materials. Plane polarized light image. E) Calcite pseudomorphs [Cal and arrows] replacing former amygdaloidal textures [Am] in volcanic rocks. F) Diverse generations of fibroradial/spherulitic chalcedony [FSC] and drusy mega-quartz cements [DM] as cavity-filling minerals. Dolomite rhombs [D] forming tiny rims around the edge of the cavities.

**Figure 3.** Borehole BH3 sedimentary log. A) Solid lines show the vertical distribution of the main sedimentologic features. Cross references to figures are written in the log. Key. Sh: Shale, C: Carbonates, V: volcanics.

**Figure 4.** A) Spherulites are composed of fibro-radial calcite generating spherical or elongated particles seen in cross Nichols. B) Volcanic remains (Volc) and spherulites (Spher) produce a floatstone texture made of clay matrix (Mg/Al clay). Calcite cements (Cem) crosscut previous materials. Plane polarized light image.

**Figure 5.** A) Thin-section of altered basaltic rock (thin section in plane polarised light). B) Composition maps showing abundance of Ca, Mg, Fe, Al, K elements within the white square on A. C) XRD analysis reveal calcite mineralogy (Cc) for the products filling cavities within altered igneous rocks.

**Figure 6.** Carbon Preference Indices of n-alkanes from the East Kirkton limestone. Equal concentrations of odd- and even- alkanes (CPI = 1) indicate full thermal maturity. It is these

measurements reflect likely liquid hydrocarbons observed in thin section to have migrated into the pore space, and that these derive from the adjacent West Lothian Oil Shale Formation.

**Figure 7.** Compilation of Sr isotope data. EK Lst indicates whole rock and HNO<sub>3</sub>-soluble fractions of 5 carbonate-rich samples from the East Kirkton Limestone Member. EK leachate / whole rock indicate whole rock and HNO<sub>3</sub>-soluble fractions of 3BH1 volcanoclastic samples. Visean Seawater data taken from (Veizer et al., 1999), hydrothermal data taken from (Palmer and Edmond, 1989) Midland Valley Volcanic series data taken from (Smedley, 1986).

**Figure 8.** Theoretical evolution of the solid mineral assemblage produced by natural hyperalkaline waters from serpentinization during ingassing of CO<sub>2</sub>. Note log scale on solid concentration axis, and linear scales otherwise. As ingassing is a progressive process, the X axis can also be read qualitatively as time or distance from source, making vertical sections of the diagram predictions of the mineral assemblage at specific water pH levels.

**Figure S1.** Facies types and stratigraphic features of the East Kirkton Quarry. A) Laminites display a flat-tabular bedding in outcrop. B) Laminites are composed of an alternation of carbonate-rich (lighter) and organic-rich laminae (darker) and are commonly displaying soft-sediment deformation features (creeping and micro-folding of laminae). C) Plant remains are common in the organic-rich intervals of laminites. D) Greenish to dark orange tuff characterised by a pyroclastic texture with mm-thick angular to subangular lapilli clasts. E)



668 Layered beds formed by an alternation of nodular to tabular limestone beds with organic-  
669 rich black clay. Slumps were present. F) Thin section of a spherulitic biohermal carbonate  
670 sample displaying the sequential stacking of mm-thick botryoidal calcite fans.

671

## SUPPLEMENTARY MATERIAL

### PHREEQC MODELLING OF SOLUTION AND MINERAL ASSEMBLAGE COMPOSITION

A simple thermodynamic equilibrium model of reactions between likely spring-water solutions arising from meteoric water serpentinization of alkali igneous rocks was created using PHREEQC Version 3.1.7. Solution composition was drawn from Stanger (1986), who report a large number of springwater compositions from the Oman Mountains. The specific site used was Jalah Spring (site 69 of Stanger, 1986), where waters rise from the middle Harzburgite of the ophiolite series (Dewandel et al., 2005). These rocks and the purely meteoric waters interacting with them provide a close match to the system inferred for East Kirkton, and therefore the solutions produced should be similar in composition. As iron and aluminium composition of these waters are not reported by Stanger 1986, we use representative values for the same region taken from Dewandel et al., (2005). Composition of the initial solution used for the model is shown in Table S1.

This initial solution was allowed to equilibrate with the minerals identified within the East Kirkton Limestone deposit (calcite, dolomite, Mg-smectite, chalcedony). In addition, the high initial pH makes it very likely that Mg-Si phases would be stable under the anticipated conditions of the experiment, so equilibration with a representative mineral (sepiolite) was also permitted (Tosca and Wright, 2015). The charge balance in solution was allowed to freely equilibrate within the parameterization of PHREEQC, and constraint of mineral stabilities was taken from the Laurence Livermore National Laboratory database (lnl.dat).

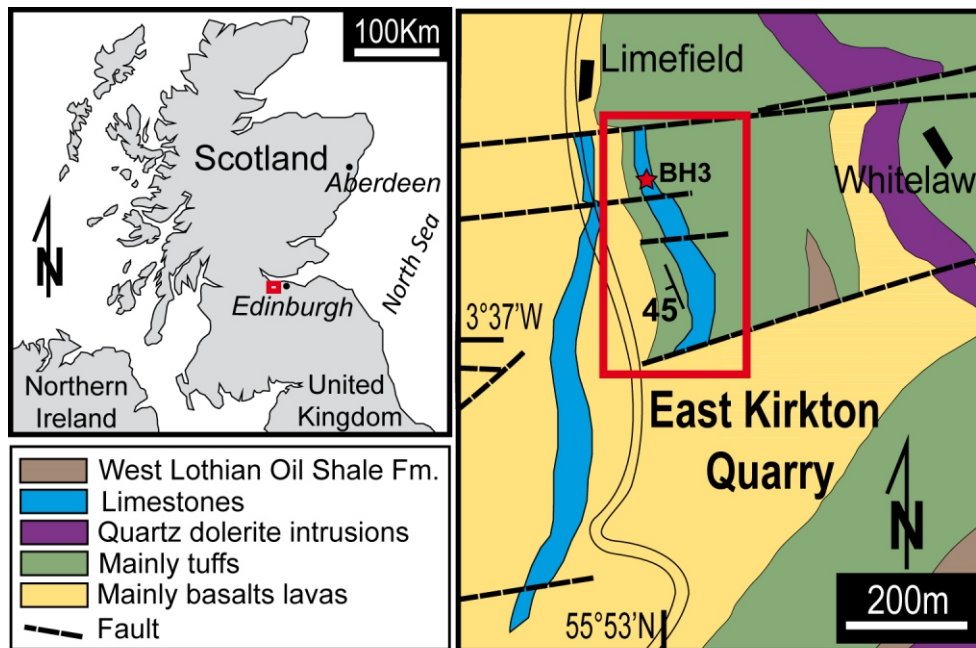
Once equilibrium between the initial solution and the permitted solid phases has occurred, reaction with gaseous CO<sub>2</sub> was incrementally achieved by sequentially adding 0.01 moles of CO<sub>2(g)</sub> and calculating the new equilibrium point, including deposition (dissolution) of solid phases. This addition of CO<sub>2(g)</sub> was continued until calcite became soluble (the abundant calcite present at East Kirkton demonstrates this threshold as not exceeded) or dissolved carbon content of the water reached 1M.

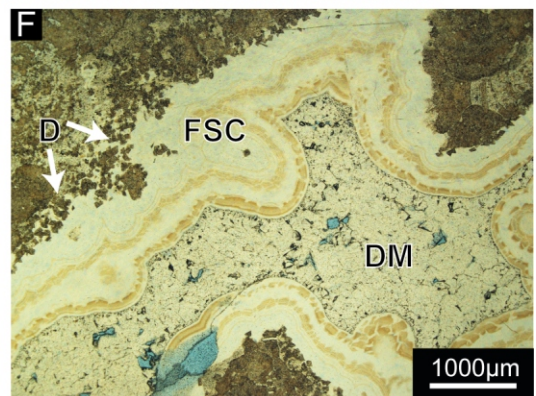
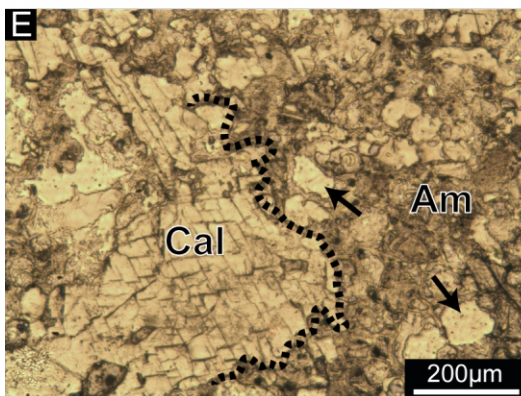
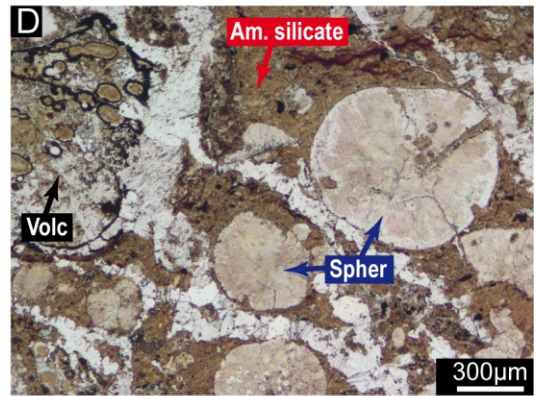
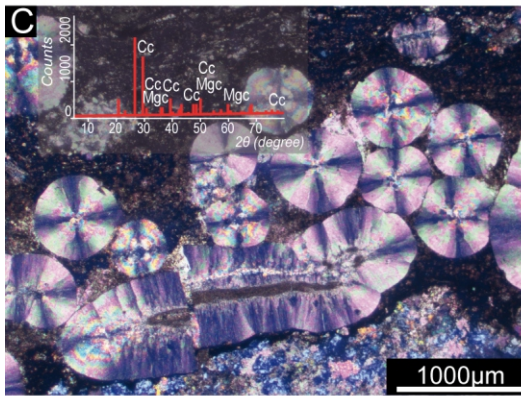
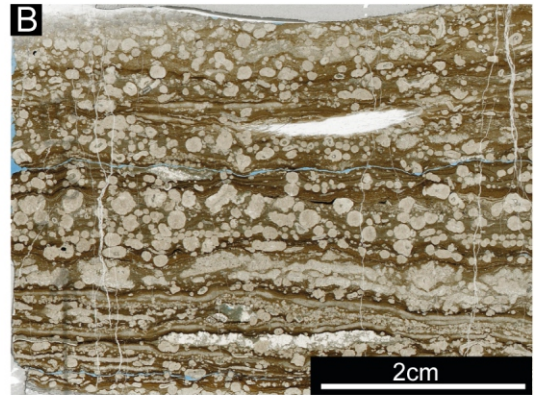
Temperature	34°C
pH	11.4
Al	0.05
Ca	1.530
Cl	11.17
Fe	4x10 <sup>-5</sup>
K	0.430
Mg	0.0017
Na	12.706
S	0.081
Si	0.568

Table S1. Composition of initial solution used for modelling. All concentrations are given in millimoles.

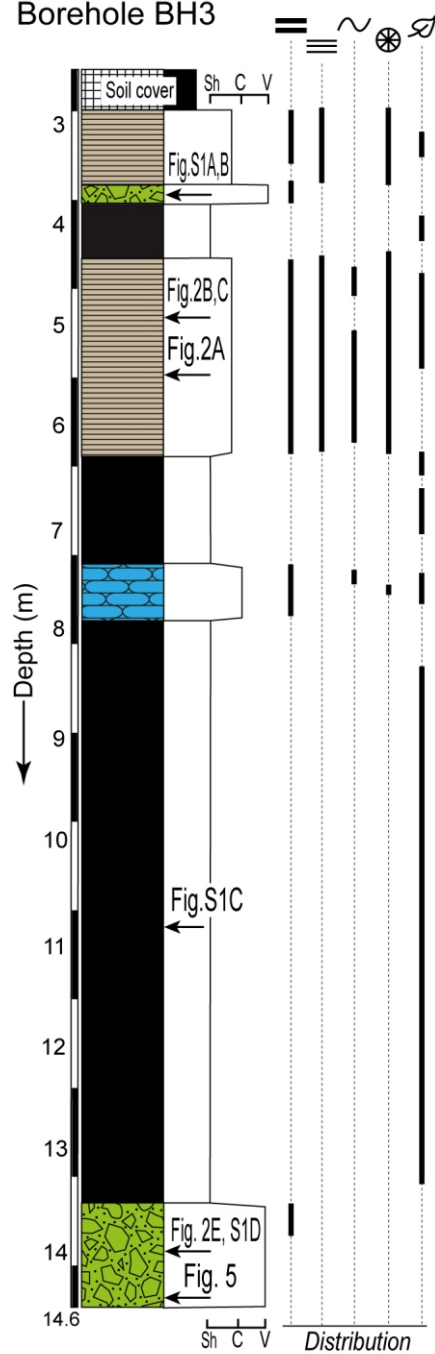
Table 1. Strontium isotope data used in this study. Position of samples shown in Figure 3. Results summarised in Figure 7.








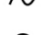

Lab No	Sample Name	Sr 87/86	% Std Error	Abs error
H639	BGS 1	0.749678	0.0013	$9.74581 \times 10^{-6}$
H640	BGS2	0.766026	0.0013	$9.95834 \times 10^{-6}$
H641	EK 0	0.706511	0.0012	$8.47813 \times 10^{-6}$
H642	EK 3	0.706817	0.0014	$9.89544 \times 10^{-6}$
H643	EK 6	0.70685	0.0015	$1.06028 \times 10^{-5}$
H644	EK 25	0.70764	0.0013	$9.19932 \times 10^{-6}$
H645	EK 30	0.706706	0.0016	$1.13073 \times 10^{-5}$
H646	BGS 1WR	0.707575	0.0015	$1.06136 \times 10^{-5}$
H647	BGS 2WR	0.708487	0.0015	$1.06273 \times 10^{-5}$
H639 leachate	BGS 1 L	0.706418	0.0017	$1.20091 \times 10^{-5}$
H640 leachate	BGS 2 L	0.706517	0.0014	$9.89124 \times 10^{-5}$



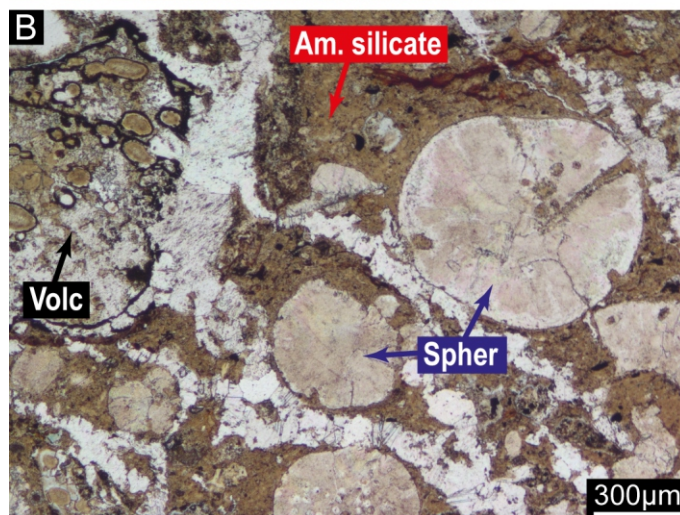
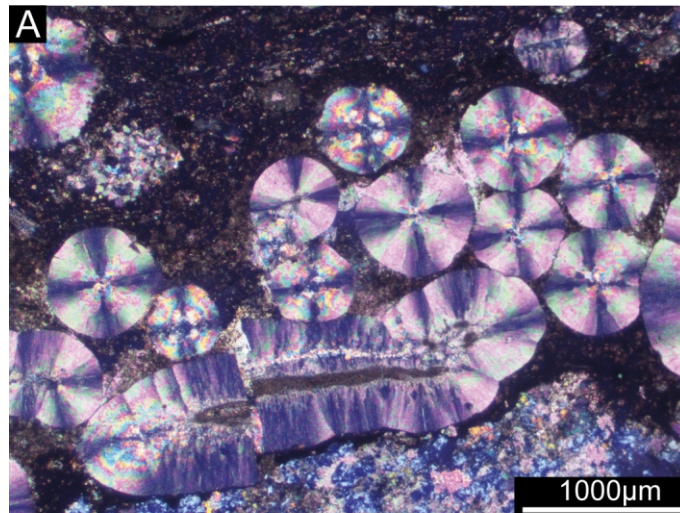


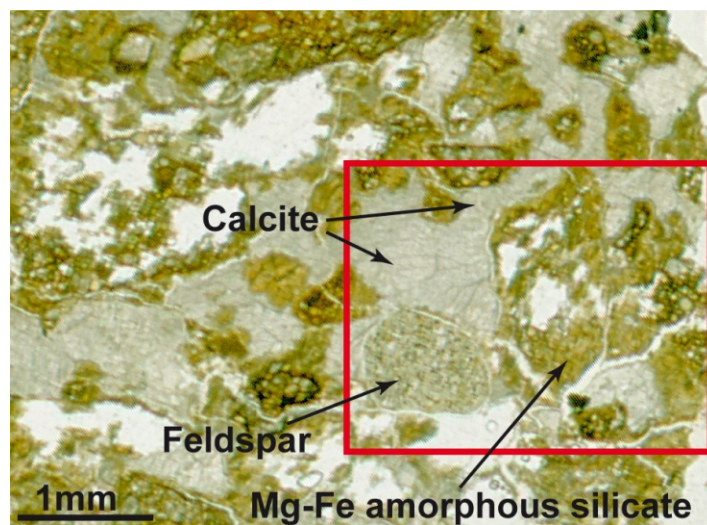
# Borehole BH3



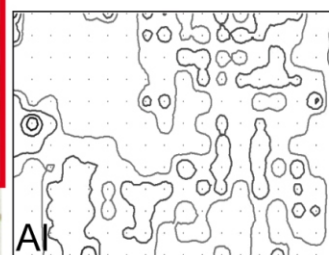
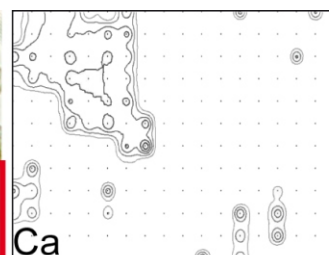
-  Tuffs
-  Layered carbonates
-  Spherulitic carbonates
-  Organic-rich shales
-  Layered beds
-  Laminites
-  Soft-sediment deformation
-  Spherulitic components
-  Organic remains



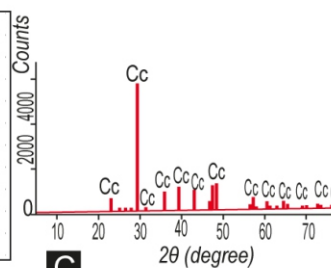
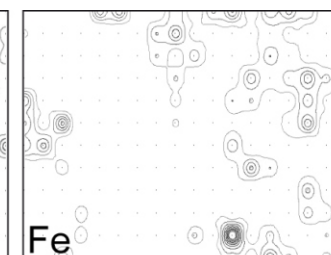
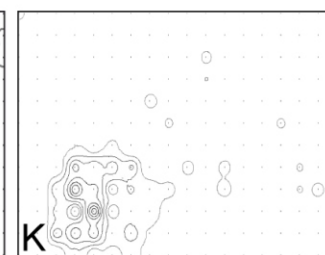
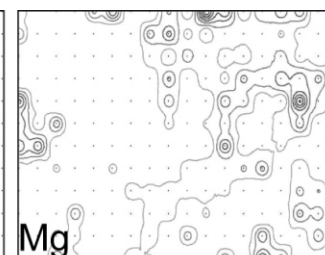




**A**



**B**



**C**



Figure 6

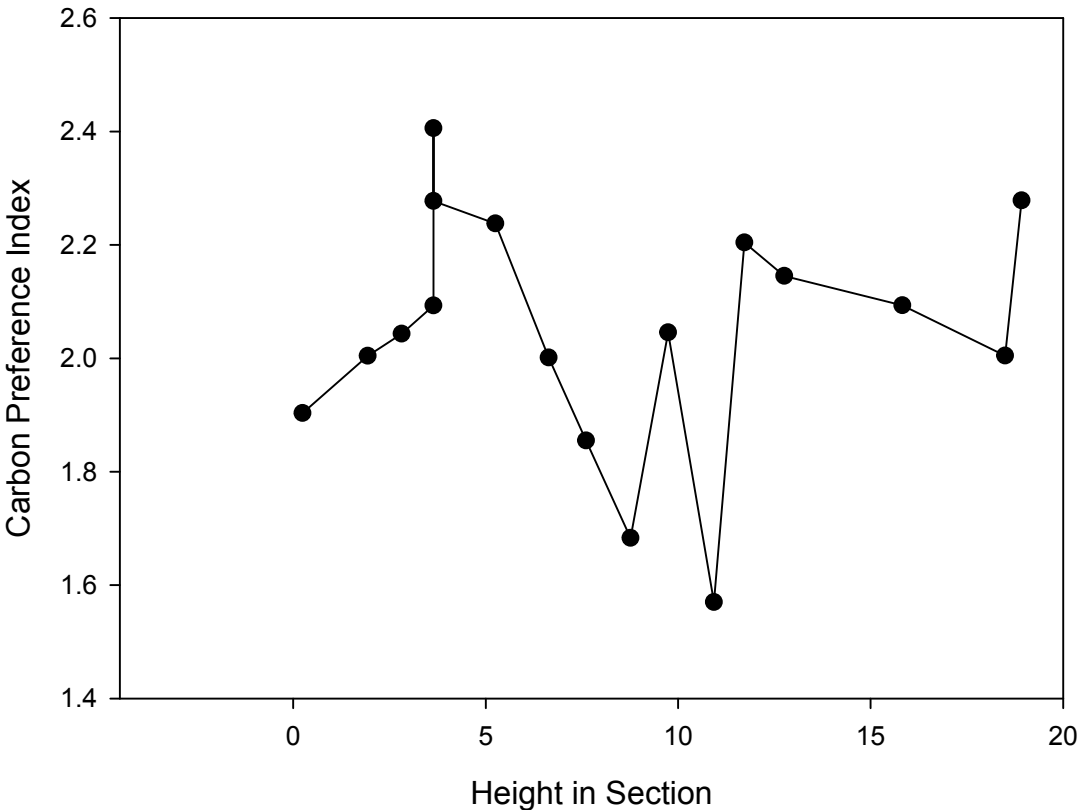


Figure 7

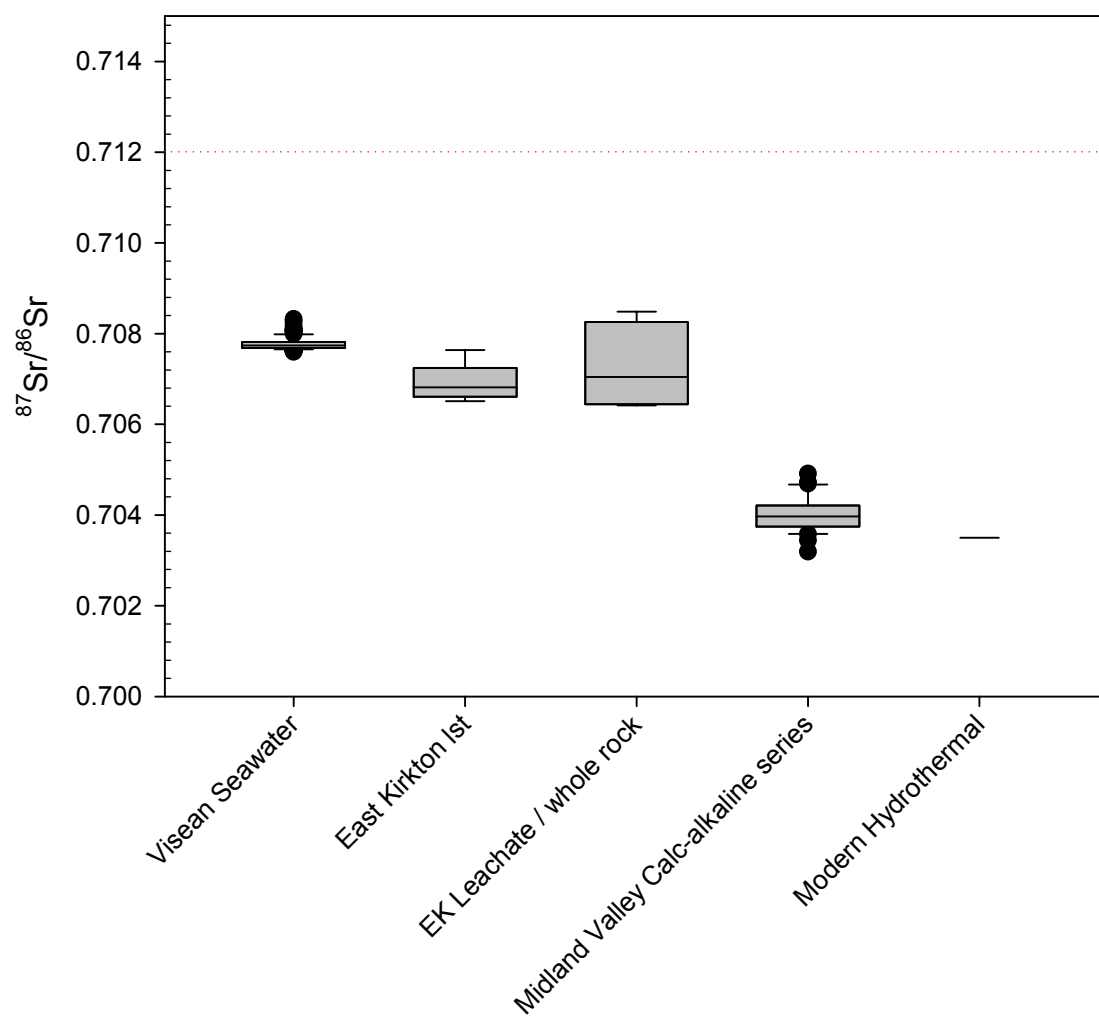


Figure 8

